Size effects in the deformation of sub-micron Au columns

Cynthia Ann Volkert, Erica T Lilleodden

Size effects in the deformation of sub-micron Au columns

Journal:	*Philosophical Magazine & Philosophical Magazine Letters*
Manuscript ID:	TPHM-05-Nov-0491.R1
Journal Selection:	Philosophical Magazine
Date Submitted by the Author:	15-Dec-2005
Complete List of Authors:	Volkert, Cynthia; Forschungszentrum Karlsruhe Lilleodden, Erica; Forschungszentrum Karlsruhe
Keywords:	plasticity of metals, compression, dislocation mechanics, focused ion beam, metals, nanomechanics
Keywords (user supplied):	

Size effects in the deformation of sub-micron Au columns

C. A. VOLKERT* and E. T. LILLEODDEN
Institut für Materialforschung II
Forschungszentrum Karlsruhe
Karlsruhe, Germany

Uniaxial compression tests have been performed on single crystal Au columns ranging in diameter from 180 nm to 8 μm. The columns were machined into the surface of a large-grained Au sheet using a focused ion beam microscope and then mechanically tested using a nanoindenter outfitted with a flat diamond punch. Images of the compressed columns show that deformation occurs by localized shear on the slip systems with the largest resolved shear stresses. After an elastic loading regime, the columns exhibit yielding in discrete strain bursts. The compressive yield stress scales roughly as the inverse square root of the column diameter. The apparent strain hardening rate also increases strongly with decreasing column diameter and stresses as large as 1 GPa are reached. Both of these size effects are attributed to dislocation source-limited behaviour in small volumes.

Keywords: Compression; Nanomechanics; Dislocation mechanics; Focused ion beam; Metals; Plasticity of metals

1. INTRODUCTION

Size effects in the mechanical behaviour of metals are of interest because of the fundamental insight they provide into dislocation mechanisms and because of their technological relevance. Metal components with sub-micron dimensions are used in many technological applications (e.g. microelectronic devices, micro-electro-mechanical devices, and nanoimprinting stamps) where mechanical integrity and reliability are paramount. For sample sizes smaller than the dislocation cell size or dislocation interaction distance (~ 5 μm) sample surface effects become very important. The importance of surfaces in deformation behaviour has been recognized for decades and has motivated studies on Au [1-3], which has no native oxide. Free surfaces can serve as effective sinks and sources for dislocations, and can inhibit dislocation storage within the deforming volume. Therefore, as sample dimensions become smaller the role of surfaces become more important, and can lead to interesting and unusual mechanical behaviour.

Nanoindentation is a useful technique for studying size effects in materials due to the ease of varying the deformation length-scale and the high resolution load-displacement data that is obtained. In the smallest depth regime, discrete displacement bursts, so called “pop-ins” [1,4-6], have often been observed and associated with dislocation nucleation events. At larger length scales, depth-dependent hardness is observed and is often described as a strain gradient effect [7]. However, the complicated, inhomogeneous strain field imposed during indentation renders such data difficult to interpret. Sample size effects have also been studied in thin film systems, where the thickness of the film is the critical length-scale. In addition to their technological relevance, the attractiveness of studying thin films is the ease of sample preparation. However, since grain size often scales with the film thickness, separating microstructure effects from sample size effects is complicated. Furthermore, for films on substrates, the substrate is inherently involved in the mechanical behaviour and where temperature changes are used to load the film, such as for wafer curvature experiments, the thermal and mechanical effects are combined. In the case of free-standing films, problems with limited ductility, buckling and tearing are often encountered.

Recently, a new approach to investigating sample size effects has been introduced [8-10]. Focused ion beam (FIB) fabrication is used to make novel micro-mechanical test specimens which can then be tested using high resolution loading such as with a nanoindenter. One particularly simple and elegant experiment involves uniaxial compression of FIB-machined columns using an nanoindenter outfitted with a flat punch. The simple loading state can be used to circumvent the strain gradients inherent in conventional indentation experiments, while still allowing isothermal, small-volume investigations. Furthermore, the fabrication of micro-columns in the surface of samples by FIB is relatively easy, site-specific, and can be applied to a wide range of materials. Since the methodology was first used to study size effects in single crystal Ni and Ni alloys [8-10], the method has been applied to <100> oriented single crystal Au [11] and in our lab to a whole range of materials such as single crystal metals (Au, Al, Cu, and Ta), multilayer films, and amorphous, nanocrystalline, and nanoporous metals.

In this paper, the compressive stress-strain behaviour of micron and sub-micron columns of single crystal Au is investigated. Using the microcompression testing method on FIB fabricated columns of varying diameter and orientation, the effect of sample size on the mechanical behaviour under uniform stresses has been systematically studied. This work goes beyond previous micro-compression work on Au [11] in that we have studied different crystallographic orientations and have achieved reliable measurements of the yield stresses in columns with diameters below 500 nm [12]. In addition to investigating size effects on the yield stress and hardening behaviour, the identification of active slip systems via post-deformation microscopy has been conducted. A new dislocation source-limited model is proposed to explain the observed inverse square root dependence of the yield stress on column diameter and the strong increase in hardening with decreasing diameter.

2. EXPERIMENTAL PROCEDURE

Gold foil with a purity of 99.999% and thickness of 100 μm was obtained in the as-rolled condition. Small pieces (3 mm by 3 mm) were mechanically polished and then annealed in vacuum at 800°C for 24 hours to allow for grain growth. The annealed foil was mounted on a SEM sample stub where it remained for all subsequent investigations. Particular care was taken when gluing the sample to the holder to avoid deformation and the introduction of dislocations in the foil. Focused ion beam (FIB) microscopy of the annealed foil revealed equiaxed grains ranging in size from 50 to 200 μm and containing occasional twin boundaries.

Three large grains (Grains A, B, and C) were selected for column preparation. The crystallographic orientations of the grains were measured using electron back-scatter diffraction and the out-of-plane orientations are described by the direction cosines h, k, and l in table 1. They all have low symmetry orientations and fall well away from the boundaries of the standard orientation triangle. This means they are expected to deform by single slip during loading in the out-of-plane direction. Crystallographic information about the three grains is given in table 1, including the Youngs moduli, and the Schmid factors and inclinations relative to the compression axis for the slip systems with the maximum resolved shear stresses.

The 30 keV Ga beam in the FIB was used to mill columns in the surface of the selected grains. The fabrication of well-defined columns with vertical sidewalls is complicated by a number of details of the ion sputtering process, namely, the finite diameter and tails of the ion beam, the angular dependence of the sputter yield, ion reflection, and redeposition. A relatively fast, two step milling method was developed to produce columns in about one hour with an approximate cylindrical geometry, as shown in figure 1. This optimised process involved first milling a ring with an outer diameter of 30 μm and an inner diameter several microns larger than the desired column diameter, to a depth close to the

desired column height. The 30 μm outer diameter is necessary to leave sufficient space for the 10 μm diameter punch that is used for mechanically testing the columns. In the second step of the milling process, a sequence of "single-pass" rings with ever decreasing radii were used to decrease the diameter of the column to the desired value. This single-pass mode results in higher sputter yields and also avoids re-deposition on the side walls of the column. From our experience, short of resorting to the effective but more time-intensive "ion lathe" method [8-10], this is the best method to minimize taper of the column walls and rounding of the top and bottom edges of the column. The geometry of the column is critical to analysing compression data, and is easily obtained from SEM imaging. The column height, h, is defined as the vertical distance between the extrapolated intersections of the inclined walls with the column top and with the underlying material (illustrated in figure 1). The column diameter, d, is defined as the diameter at half the column height. Final column diameters ranged from 180 nm to 8 μm and heights from 500 nm to 11 μm. The aspect ratios of the columns were chosen between 1.5 and 4. Below 1.5, there is danger that slip may be hindered by the underlying material. Above an aspect ratio of 4, plastic buckling of the columns becomes a problem. A constant aspect ratio also ensures a constant fractional contribution from constraints at the column ends and from the compliance of the underlying material [13].

The columns were compressed in an MTS XP Nanoindenter using a flat diamond punch. The punch is a 60° conical indenter that has been truncated to form a 10 μm diameter circular flat (Synton, Switzerland). A typical experiment consisted of compressing the column at a fixed loading rate (between 0.8 and 100 μN/s) to a prescribed maximum displacement, followed by a hold-load segment prior to unloading.

The stress and strain in the column is determined using the measured force on the column F and the measured displacement Δx_{meas} into the sample surface. Given the fact that deformation often occurred inhomogeneously by single or double slip, determination of the true stresses and strains was not attempted and the engineering stresses $\sigma = 4F/\pi d^2$ and engineering strains $\varepsilon = \Delta x/h$ of the columns were used instead. However, an important correction to the displacement data due to the compliance of the underlying material is needed [13,14]. Assuming that the displacement profile of the material under the column can be approximated by the displacement profile due to pushing a rigid punch into the surface, the relation between the column displacement Δx and the measured displacement Δx_{meas} is [14],

$$\Delta x = \Delta x_{meas} / (1+ (\pi/4)(1-\nu^2)(d/h))$$

where ν is the Poisson ratio of the underlying material (0.44 for polycrystalline Au) and h/d is the column aspect ratio. For the smallest column aspect ratio of 1.5 the contribution to the measured displacement from the underlying material ($1-\Delta x/\Delta x_{meas}$) can be as large as 30%. This correction does not account for possible plasticity in the underlying material, which can lead to apparent decreases in the measured stresses and increases in the plastic strain. However, we do not believe that plasticity in the underlying material is a major issue since the total plastic strain measured with the nanoindenter (after unloading) is consistent with the total change in column height observed in the SEM, to within several percent strain. Other known inaccuracies in the engineering stress and strain calculated as described above come from deviations in the column geometry from a perfect cylindrical column (e.g., column taper), possible friction between the diamond punch and the column top, and constraint of the column by the underlying material [13]. For the column shapes used here, these effects are deemed negligible in comparison with the assumptions associated with using the engineering stress and strain.

Following compression, the deformed columns were imaged by SEM. In addition to qualifying the type of slip that occurred (e.g., single or multiple slip) and identifying the active slip systems, SEM imaging allows verification that the column was contacted and not

the surrounding material. Although it was not always apparent from the stress-strain curves, SEM images showed that some of the columns deformed by plastic buckling; these columns were not considered in subsequent analysis.

3. EXPERIMENTAL RESULTS

An engineering stress-strain curve is shown in figure 2 from a 710 nm diameter column with an initial height of 1.75 μm. The column deformed by single slip as evidenced by the post-compression SEM image in the inset of the figure. The inclination of the slip plane to the load axis can be estimated as 52° which is the predicted inclination for the active slip system in this grain (table 1). The steep increase in stress at the beginning of the loading cycle is due to elastic loading in combination with "early plasticity" effects. Such micro-plasticity is likely due to surface roughness and initial seating of the punch on the top of the column; perfect planarity between the punch and the column is not achievable. At larger strains, the column deforms plastically in discrete strain bursts separated by almost elastic loading intervals. At the maximum depth of 400 nm, the measured load is held fixed for 15 s. The beginning of the hold is indicated by an arrow in figure 3 during which time one percent plastic strain occurs. The slope of the first part of the unloading curve is 109 GPa, which is larger than the calculated value of the Youngs modulus for this orientation (table 1). This presumably has to do with the change in column geometry due to deformation. Estimating the deformed column geometry from the image in figure 2 (1.6 μm height, 800 nm diameter), the corrected Youngs modulus becomes 79 GPa, which is very close to the expected value (table 1).

Here we define the yield stress for the columns as the stress at 5% plastic strain since the usual definition of yield stress at 0.2% plastic strain is difficult to apply to these experiments due to early plasticity. By selecting a plastic strain of 5%, one can minimize errors due to early plasticity while still avoiding extensive strain hardening effects in the yield stress. The amount of strain hardening is estimated from the slope of the data between 5 and 15 % plastic strain or until the end of the loading curve. For the 710 nm column, the yield stress is 154 MPa and the strain hardening coefficient is 472 MPa.

Representative stress-strain curves for columns with different diameters are shown in figure 3. Both the yield stress and the strain hardening coefficient increase with decreasing column diameter. SEM images of the deformed columns are shown in figure 4. Single slip (figure 4(c) and (f)) and multiple slip (figure 4(a), (b), (d), and (e)) are seen. In some cases deformation is localized in a few narrow slip bands (figure 4(c) and (f)), in other cases numerous slip bands are formed (figure 4(a) and (b)). The column in figure 4(e) shows an example of homogenous duplex slip followed by localized single slip on a third system. The number of active slip systems did not depend on column diameter but did depend on the crystallographic orientation: most of the columns fabricated within Grain A deformed by double or triple slip, most of the columns fabricated within Grain B deformed by single slip, and all of the columns fabricated within Grain C exhibited double or triple slip. This is consistent with the resolved shear stresses. The primary slip systems have a Schmid factor of 0.48 in all grains. The second highest Schmid factor is 0.44 in Grain A, 0.40 in Grain C, and 0.38 in Grain B. In all grains, estimates of the inclinations of the slip planes from the images are consistent with slip occurring on the systems with the highest resolved shear stresses.

To illustrate the extent of the reproducibility of the stress-strain behaviour, the loading data from six 300 nm diameter columns are shown in figure 5. Allowing for early plasticity and the stochastic nature of the strain bursts, the curves agree quite well. Additionally, strain rate sensitivity was not observed; columns tested at different loading rates showed nominally the same stress-strain response. The deformed columns corresponding to the curves labelled (a) – (c) in figure 5 are shown in figure 6. The columns from Grain A (figure 6(a) and (b)) show very localized slip on one slip system and more homogeneous slip on a second system.

Column (b) deforms at a larger stress than column (a) and along a slip system at the bottom of the column with a longer slip path. The slip geometry of the column from Grain C (figure 6(c)) is probably localized single slip although it is difficult to see due to the presence of a partially decohered and burst surface film. This surface film is believed to be a carbon-based layer that forms during SEM imaging of the Au columns prior to mechanical testing and that typically bursts or delaminates during testing. In larger columns where smaller electron beam fluences are needed for imaging or in columns that were imaged with the ion beam no evidence of a surface layer was found. For this reason, it is concluded that the approximately 20 nm thick layer is carbon-based and is deposited during electron beam imaging. No difference was observed between the mechanical behaviour of columns with and without the carbonaceous layer (e.g. figure 5).

The yield stresses and the strain hardening rates are summarized in log-log plots in figure 7 for all of the columns tested. Both quantities increase strongly as the column diameter is decreased from 8 μm to 180 nm. No obvious differences are observed between the yield stresses and strain hardening rates for the different grain orientations, revealing that the stress-strain behaviour does not depend strongly on whether single or multiple slip occurs.

4. DISCUSSION

A systematic investigation of the stress-strain behaviour and deformation morphology of small Au columns under uniaxial compression has been performed. It is observed that plastic deformation occurs largely by discrete strain bursts associated with dislocation glide on the slip systems with the maximum resolved shear stresses. The resultant stress-strain behaviour does not depend on whether single or multiple slip occurs or whether it is localized or homogeneous. This somewhat surprising result can be rationalized by the easy egression of dislocations through the surfaces of the smaller columns; dislocation storage is insignificant, therefore the typical hardening response from secondary slip is not observed.

Discrete strain bursts during homogeneous loading were first observed in Ni and Ni alloy columns [8-10] and have also been reported in <100> Au columns [11]. They are similar in concept but larger than the strain bursts observed during inhomogeneous loading by nanoindentation of a wide range of metals [15]. Presumably, the strain bursts are due to a plastic instability or self-organized critical behaviour [15], where the motion of a few individual dislocation sets off an avalanche of dislocation nucleation and glide events. For example, the motion of roughly 400 edge dislocations to the sample surface within less than one second would be required to explain the strain bursts observed in the 710 nm diameter column in figure 2. The magnitude of this effect is certainly enhanced by the load control used in these experiments since the stress is held almost constant during such a burst. While the load control testing procedure influences the strain bursts it is not believed to be the origin of the effect.

A best fit to the yield stress data (figure 7(a)) gives $\sigma_y \sim d^{-0.61}$ which is close to the inverse square root dependence typically observed for the effect of grain size on yield stress (e.g., the Hall-Petch relation). In the largest columns, yield stresses as small as 50 MPa are measured, falling between the values for the yield stress of well-annealed (~2 MPa [16]) and severely worked (205 MPa [17]) bulk, single crystal Au. In the smallest column (180 nm diameter), a yield stress of 560 MPa is reached. The data measured here agree well with polycrystalline Au film data obtained at much lower strains by wafer curvature measurements during thermal cycling [2] (shown in figure 7(a)) and with previous data for <100> Au columns with diameters above 500 nm [11]. In contrast, the tremendously large yield stresses measured by Greer et al. [11] in <100> oriented Au columns with diameters smaller than 500 nm are not observed here. It has since been acknowledged [12] that these high yield stresses were not accurately analysed.

The strain hardening rate (figure 7(b)) is best described by the relation $E_h \sim d^{-1.07}$. The rate determined using the "true" stresses and strains (defined as the instantaneous stress and strain assuming homogeneous deformation and volume conservation) will certainly be lower than that for the equivalent engineering stress and strain response used here. However, due to the inhomogeneous nature of the deformation in most of the columns tested here, estimates of the strain hardening rate based on the true stress and strain are not expected to be any more accurate than those based on the engineering stresses and strains. For instance, localized plasticity on a single slip plane would lead to a reduction in the cross sectional area, rather than an increase as would be predicted from a volume conservation assumption used in true stress-strain analyses [11]. In addition, although a more accurate determination of the stresses and strains might lead to lower values of the strain hardening rate, it will not eliminate the very strong effect of column diameter. The strain hardening rate in the largest columns is roughly 100 MPa which agrees very well with the values for hardening in bulk metals. In the smallest columns, the large strain hardening rates of 5 GPa result in stresses close to the theoretical strength (roughly 2 GPa for Au of this orientation [18]) being reached. The column that showed the largest stress of 1 GPa (figure 6(b)) exhibited homogeneous slip on one slip system followed by very localized slip at the base of the column on a second slip system. In order to reach the large stresses necessary to activate this second slip system, the sources on the first system must have been depleted.

Three different mechanistic scenarios are discussed to account for the observed dependence of the yield stress and strain hardening rate on column diameter. These are: (1) Taylor hardening by dislocation interactions, (2) the presence of a surface layer that acts as a barrier to dislocation motion, and (3) dislocation source-limited behaviour.

(1) The classic explanation for an increase in yield stress is through an increase in dislocation density (Taylor hardening). As the dislocation density is increased, the stress required to move a dislocation through a field of dislocations is also increased. However, to reach the measured stresses of more than 1 GPa, a dislocation density of $10^{16}/m^2$ is required (dislocation spacing of 10 nm). Such high dislocation densities are only observed in deformation cell walls and are not expected to be reached here. In addition, the observed yield stress dependence on the column diameter would require that the dislocation density scale as the inverse of the diameter. This is often predicted for sample volumes with blocking boundaries [19-21]. However such a situation is hard to envision if the dislocations are free to leave through the surface. In fact a recent two-dimensional simulation of the dislocation density in small compression specimens with free surfaces predicts that the dislocation density scales directly as the square root of the sample diameter [22]. With or without a blocking surface layer, it is hard to envision reaching the high dislocation densities necessary to explain the large measured stresses by Taylor hardening.

(2) It is usually assumed that the Au surface is oxide-free and that dislocations can easily leave the crystal helped by image forces. The surface carbonaceous film associated with electron beam imaging discussed earlier does not influence the stress-strain behaviour and presumably does not hinder dislocation motion. However in the columns studied here, fabrication by Ga ion beam sputtering will result in a heavily damaged, implanted layer at the side walls of the columns. Based on Monte Carlo simulations [23] of 30 keV Ga sputtering of Au at a glancing angle of 2°, both ion beam damage and several atomic percent of Ga are expected in the outer 15 nm of the sample. If the layer is sufficiently strong and stiff to block the egress of dislocations from the sample, then deformation is expected to occur by the nucleation and pile up of dislocations in the Au column until stresses are reached that are large enough to break through the alloy surface layer. By analogy with the mechanism proposed for the Hall-Petch relation in polycrystalline samples, as well as based on discrete dislocation simulations of dislocation nucleation in bounded volumes [24], it is expected that a blocking surface layer will lead to an inverse square root dependence of the yield stress on

the column diameter, consistent with the observations presented here. Under certain circumstances, blocking boundaries can also lead to a significant increase in strain hardening with decreasing sample size [19]. However, although the presence of a hard surface layer is consistent with the results presented here, it is unlikely that the Ga-implanted layer can support such large stresses or that sufficiently high dislocation densities can be reached, as discussed in point (1).

(3) A third and more convincing rationale for the observed size dependence can be found in dislocation source-limited behaviour. Following the framework of the Hall-Petch relation, a large dislocation density (such as in a dislocation pile-up) leads to large internal stresses which can activate dislocation sources. Since the dislocation density is expected to be lower in the small columns due to the loss of dislocations through the sample surface, the applied stress required to nucleate or activate dislocation sources can be argued to decrease with increasing column diameter. Thus, large columns will have a high dislocation density and will readily reach the local stresses required to nucleate or activate sources. In contrast, the small columns will have a lower dislocation density and will require applied stresses closer to the theoretical source strength to deform. According to Hall-Petch considerations as well as discrete dislocation simulations [22], this will lead to an inverse square root dependence of the yield stress on the column diameter, as is observed. As plasticity continues, the dislocation density is further reduced by dislocations leaving the crystal through the surface, which happens preferentially in the smallest columns. This in turn requires an increase in applied stress to activate new sources. This hardening mechanism is therefore due to a *decrease* in dislocation density rather than an *increase* as described by the conventional Taylor model. Thus, the dislocation source-limited model is able to qualitatively account for the dependence of the yield stress on column diameter and the increase in strain hardening with decreasing column diameter.

5. CONCLUSIONS

We have performed compression tests on micron and sub-micron single crystal Au columns. Plastic deformation occurs by bursts of gliding dislocations on the slip systems with the maximum resolved shear stresses. Both the yield stress and apparent strain hardening rate increase strongly with decreasing column diameter and are not strongly influenced by the number of active slip systems. The density of dislocations required to account for the observed stresses by Taylor hardening are unrealistically high. Also, it seems unlikely that the Ga damaged surface layer created in these columns during fabrication will have the strength to block dislocation motion at the stresses observed here. Thus, it is concluded that the most likely explanation for the observed dependence of the mechanical behaviour on column diameter is that deformation is controlled by the activation of dislocation sources. As the column size is decreased or as the plastic strain is increased, dislocations are lost through the sample surface and the dislocation density is decreased. The decrease in dislocation density results in an increase in the applied stress necessary for further plasticity by dislocation source activation and is proposed to account for the observed yield stress and strain hardening behaviour.

ACKNOWLEDGEMENTS

One of us (ETL) gratefully acknowledges support from the Alexander von Humboldt Foundation.

REFERENCES

Volkert - Figure 1

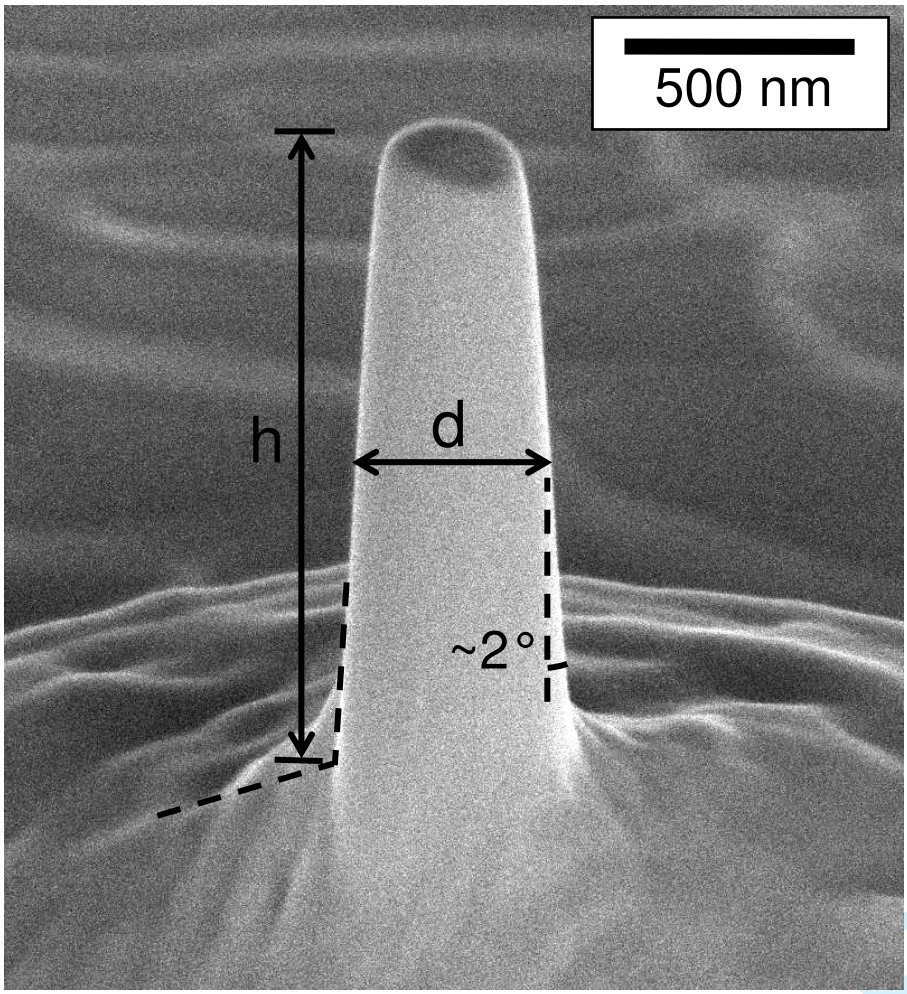

Volkert - Figure 2

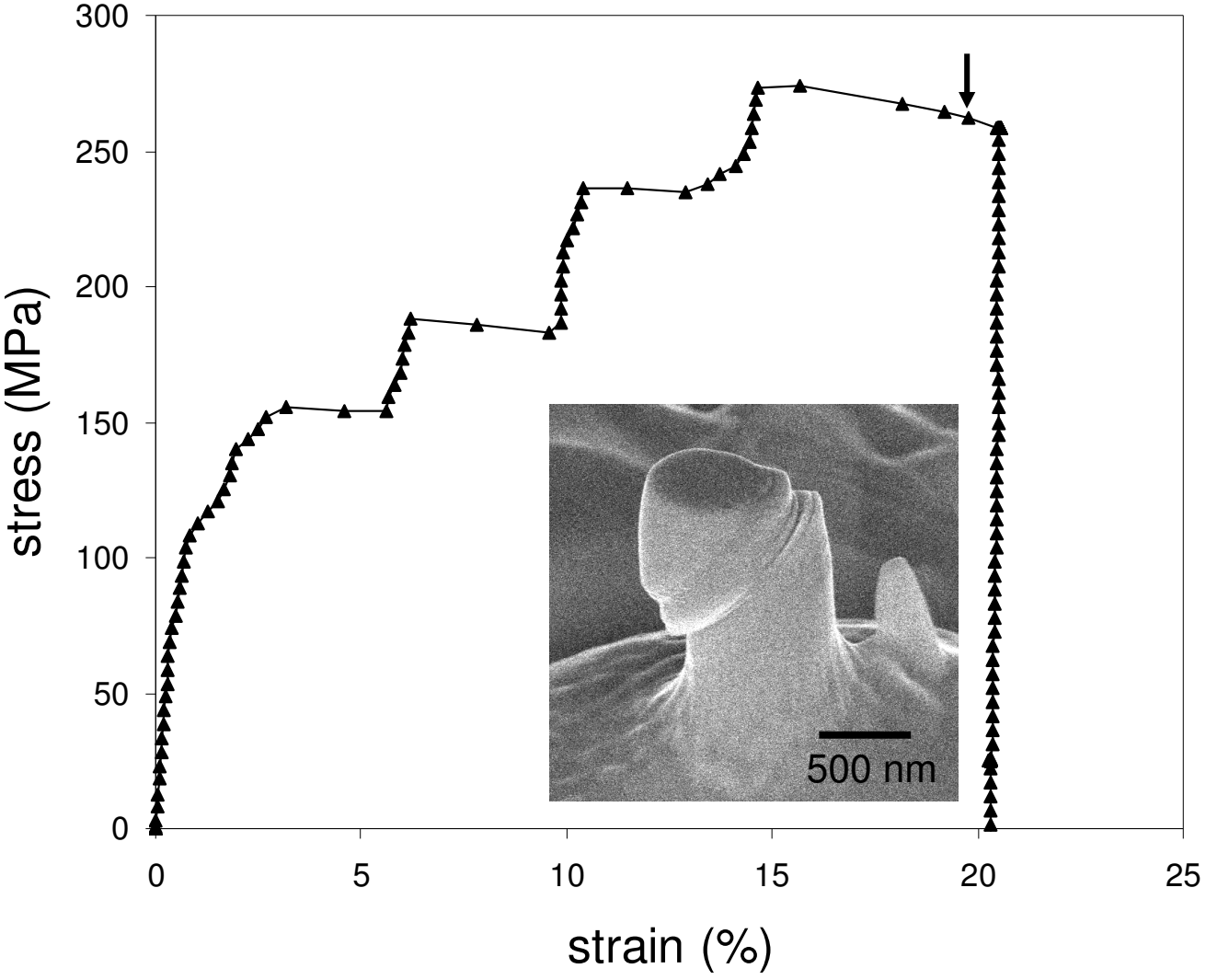

Volkert - Figure 3

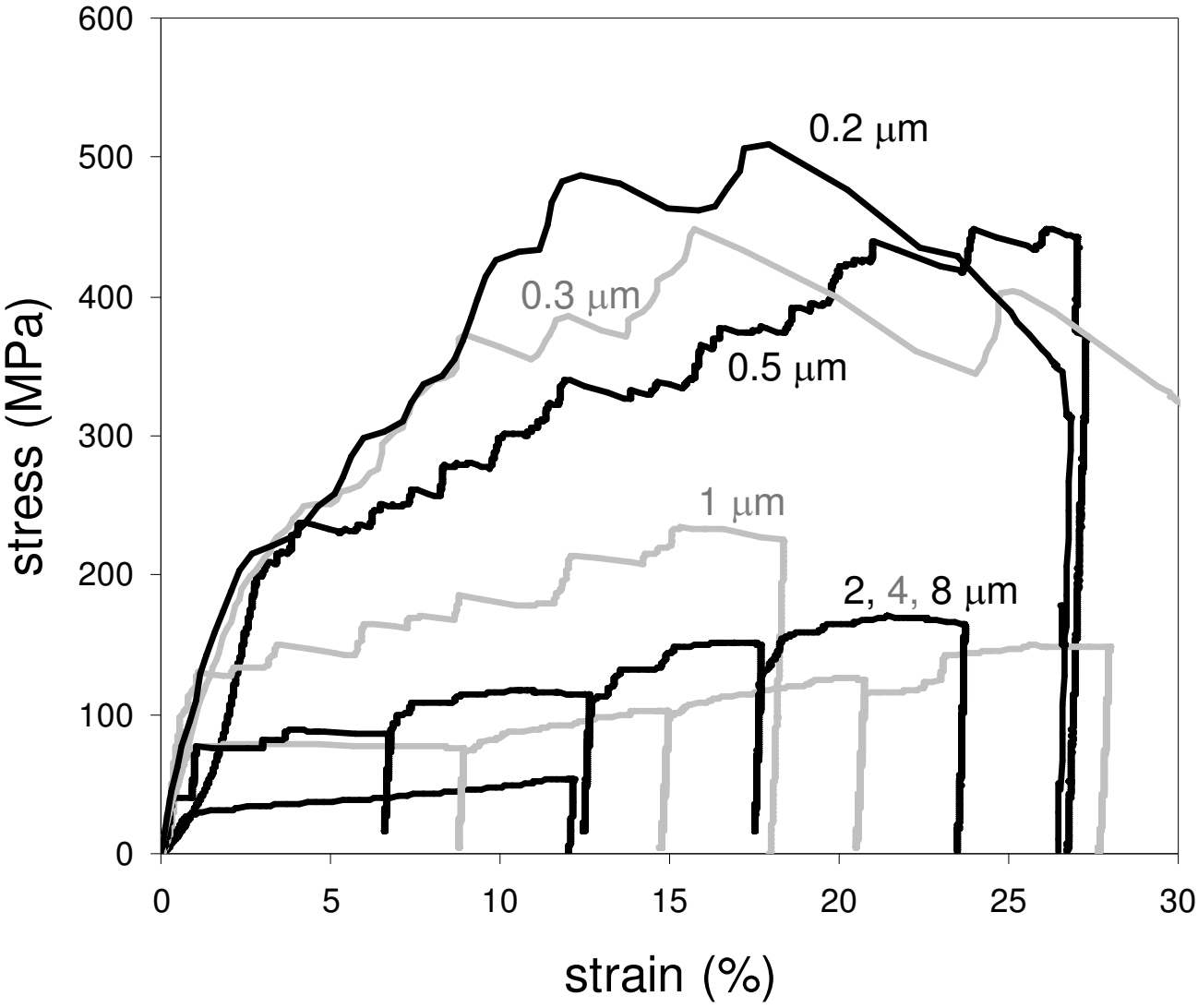

Volkert - Figure 4

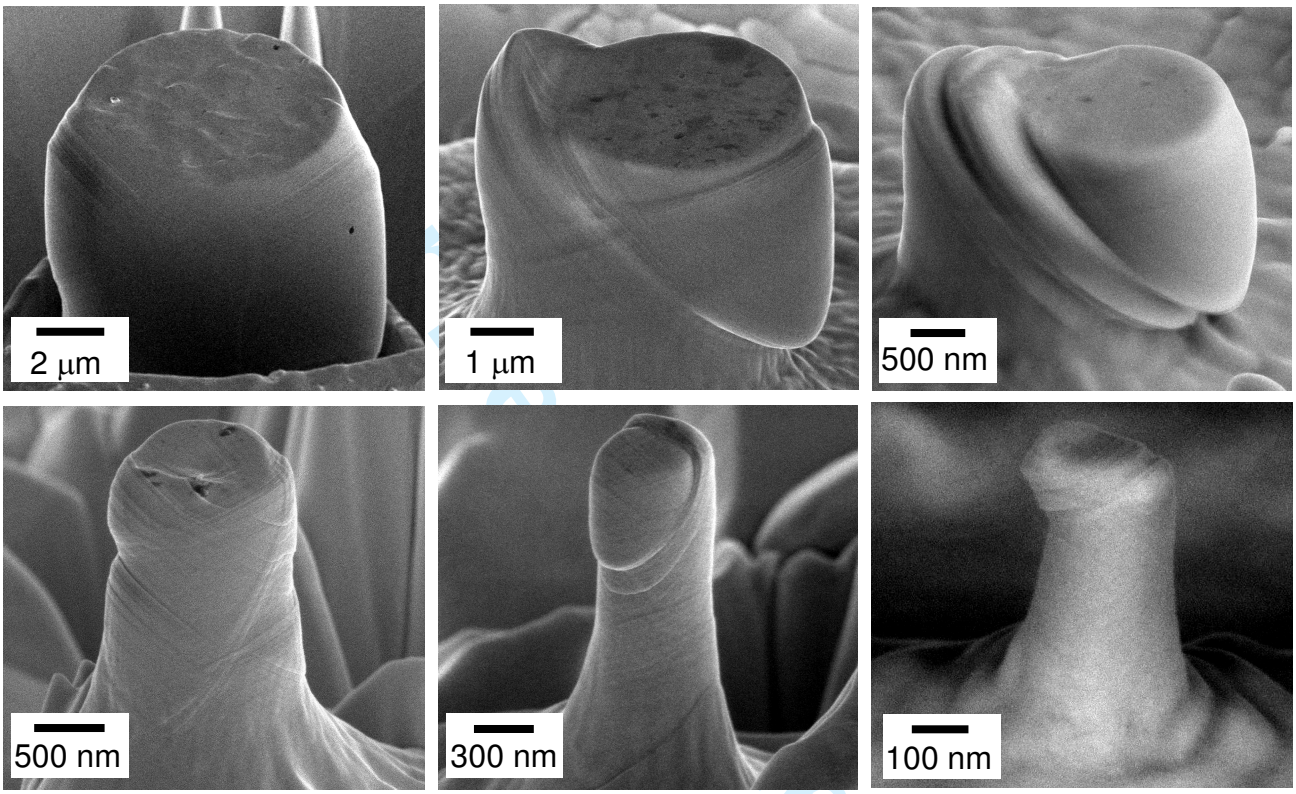

Volkert - Figure 5

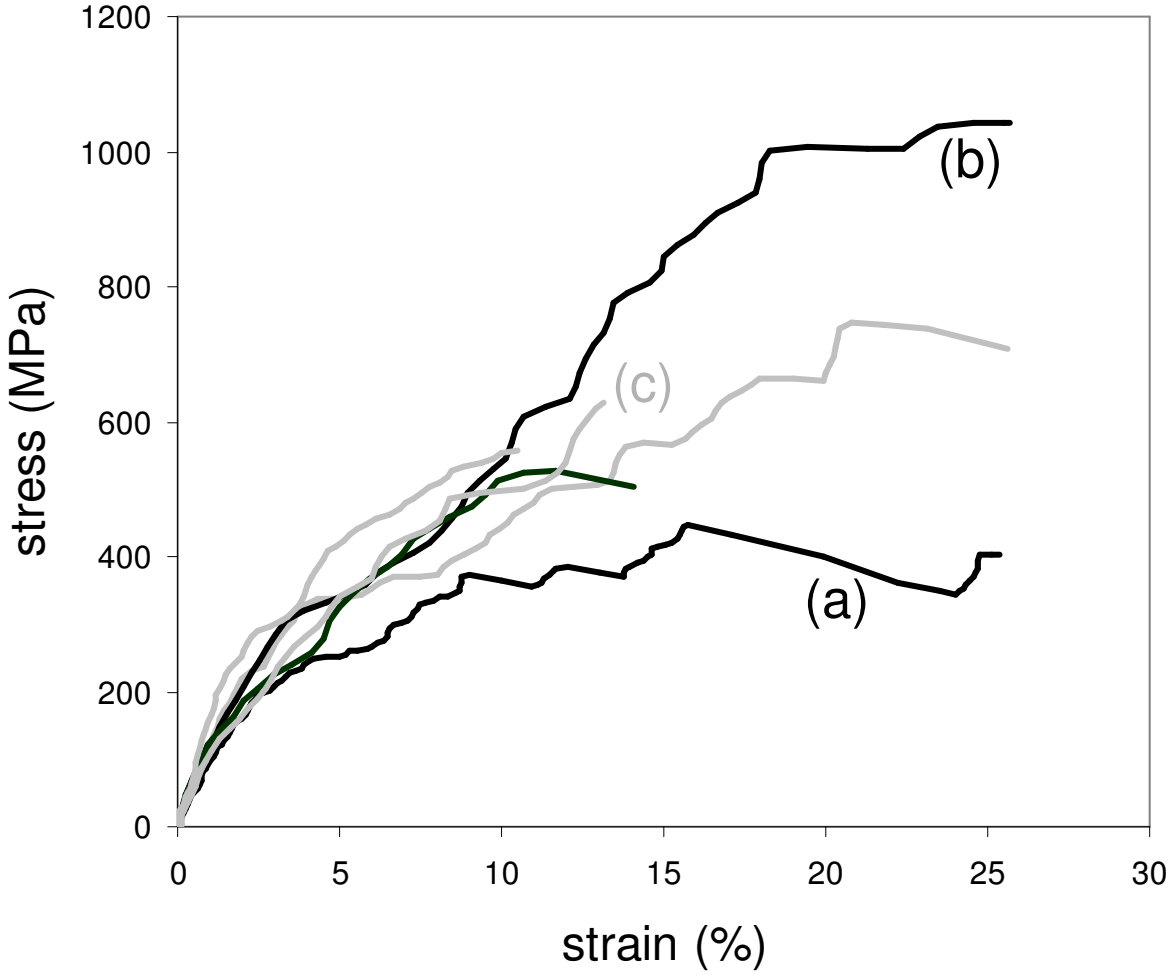

Volkert - Figure 6

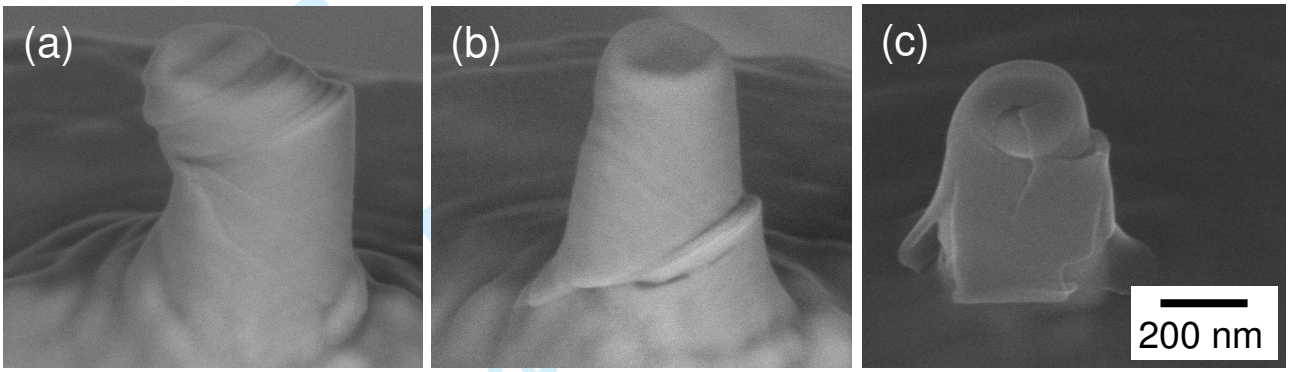

Volkert - Figure 7